Asian Journal of Chemistry; Vol. 37, No. 7 (2025), 1736-1742

ASIAN JOURNAL OF CHEMISTRY

https://doi.org/10.14233/ajchem.2025.33574

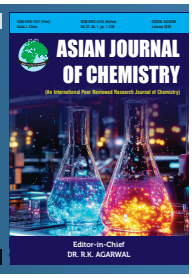

Synthesis of Molecularly Imprinted Polymers for the Extraction of *p*-Hydroxybenzoic Acid

SHOWKAT AHMAD BHAWANI*, AQIL FAIZ MOHAMAD RAMEZAN, RACHEL MARCELLA ROLAND, MOHAMAD AIMAN OTHMAN and ALDRIN FELIX SIMBAS

Faculty of Resource Science and Technology, Universiti Malaysia Sarawak, Kota Samarahan, Sarawak-94300, Malaysia

*Corresponding author: E-mail: sabhawani@gmail.com

Received: 20 February 2025; *Accepted*: 18 June 2025; *Published online*: 30 June 2025; AJC-22050

p-Hydroxybenzoic acid (*p*-HBA) is widely found in the environment due of its exceptional properties and has been used in the synthesis of variety of products such as preservatives, dyes, bactericides, *etc*. This causes a huge disposal of *p*-HBA in the environment which is considered to be harmful to both aquatic and terrestrial life. The molecular imprinting technique was employed to fabricate a molecularly imprinted polymer (MIP) that possesses selective binding sites for the *p*-HBA. In this study, *p*-HBA was used as the template molecule for the MIP synthesis, which was carried out using the precipitation polymerization method with a non-covalent approach. Acrylic acid was employed as the functional monomer, while ethylene glycol dimethylacrylate (EGDMA) was utilized as the cross-linker. The characterization of the MIP of *p*-HBA was conducted with scanning electron microscopy (SEM) and Fourier transform infrared (FTIR). The SEM results showed that both MIP and the non-imprinted polymer (NIP) of *p*-HBA were spherical in shape. The MIP attained its highest efficiency at optimum conditions of 1 ppm initial concentration, 0.4 g of polymer dosage and 210 min contact time. Moreover, the competitive binding assay indicated that the MIP displayed a greater affinity towards *p*-HBA than benzoic acid. The synthesized MIP was successfully used for the extraction *p*-HBA from blood serum and the extraction efficiency was about 80.56%.

Keywords: *p*-Hydroxybenzoic acid, Molecularly imprinting polymer, Blood serum.

INTRODUCTION

p-Hydroxybenzoic acid (*p*-HBA) acid is one of the phenolic acid compounds occurs naturally in various plants which can be found in fruits, vegetables and some medicinal plants. For example, plants like soybean, corn, rice and wheat contains *p*-HBA, which can be obtained from their root exudates [1]. Generally, *p*-HBA has been utilized for various applications such as an antioxidant, preservative and fungicide in foods, beverages, medicines and cosmetics [2,3]. It has been proved that the insertion of *p*-HBA into the chitosan molecule had increased its antioxidant and antibacterial capabilities [4]. Once penetrating in the environment such as in soils, sediments and water systems, *p*-HBA can become extremely persistent [5,6]. The *p*-HBA may be harmful to humans, animals and plants [7,8] because it has also been detected in food, crops and human urine [9,10]. One major contributing factor to nutrient deficiencies, for instance, is high *p*-HBA in soils, which inhibits plant growth and reduces agricultural output [11]. However, *p*-HBA is also known as allelochemical [12], which tends to affect soil health [13] and hinder plant growth [14,15]. This is because it can directly control the activities of the metabolic enzymes within the glycolysis and pentose phosphate oxidation and hence, leads to the suppression of seed germination and root growth [16,17]. Besides that, *p*-HBA also impeded plants' carbon and nitrogen metabolism and caused damage to the DNA and proteins within the plants [18,19]. The application of *p*-HBA reduced the expression of genes related to the cell cycle and decreased the length of mature root cells in cucumber roots [20].

Moreover, exposure to *p*-HBA led to alterations in photosynthesis, respiration and genes associated with reactive oxygen species in the leaves of *Populus* × *euramericana* "Neva" [21]. In addition, it has adverse effects on humans when *p*-HBA is used in cosmetics or pharmaceutical products including skin irritation, eye irritation and respiratory tract irritation. *p*-HBA is derived from the hydrolysis of parabens, a commonly used preservative in cosmetics and food products [22,23]. Though *p*-HBA is not acutely toxic, it still exhibits estrogenic activity, promoting the growth of human breast cancer and is regarded

as a biomarker for gastric cancer [23-26]. In order to prevent *p*-HBA from being consumed and from piling up in the human body, it is imperative that the concentration of *p*-HBA in foods and environments be reduced. Therefore, it is necessary to monitor *p*-HBA with a well-established method.

Molecularly imprinted polymers (MIPs) are versatile materials for the extraction of *p*-HBA from any sample because it is designed with characteristics of high affinity and selectivity towards its target molecule [27]. Basically, MIPs are prepared by mixing template molecule, functional monomer, cross-linker, initiator and solvent together to become a pre-polymerization mixture, which then will undergo a polymerization reaction at optimized time and temperature and later the products of polymerization undergo template removal to obtain MIPs containing highly specific and selective binding sites [28]. MIPs can be synthesized by various methods including bulk polymerization, precipitation polymerization, emulsion polymerization, suspension polymerization and dispersion polymerization. Among these, bulk polymerization is the most conventional method that produces bulk monolith [29] while precipitation polymerization is the most popular method to produce micro spherical polymer particles [30-32]. This is because the MIP preparation method is easy and cheap, as well as the produced MIPs are stable and can resist extreme temperature and harsh chemical media [33]. A few studies have been reported for the development of MIPs for *p*-hydroxybenzoic acid (*p*-HBA) as a template molecule and their recognition and separation performances were assessed [34-38]. In this study, acrylic acid was used to establish an interaction with the *p*-HBA through non-covalent bonding and a precipitation polymerization technique was used to complete the polymerization reaction.

EXPERIMENTAL

p-Hydroxybenzoic acid (*p*-HBA), benzoic acid, ethylene glycol dimethylacrylate (EGDMA) were purchased from Sigma-Aldrich Co. Ltd. (USA). The other chemicals like acrylic acid (AA), acetonitrile (ACN), azo-*bis*-isobutyronitrile (AIBN), methanol, acetic acid, acetone were procured different commercial chemical suppliers.

Synthesis of MIP: The molecularly imprinted polymer (MIP) of *p*-HBA was prepared by precipitation polymerization techniques with a non-covalent approach [31]. In the preparation of MIP, the template (*p*-HBA), monomer (AA) and cross-linker (EGDMA) were used in the ratio of 1:3:12, respectively. Firstly, the template was dissolved in 75 mL of acetonitrile in a reaction flask and then monomer and cross-linker were added in the reaction mixture. After that, a 0.03 g AIBN as an initiator was added to initiate the polymerization process. The mixture was sonicated for 15 min and then purged with nitrogen for 15 min. After this process, the reaction flask was sealed and kept in a water bath at 60 ºC for 2 h and 80 ºC for 4 h. The synthesized polymer beads were collected and washed with methanol to remove unreacted materials on the polymer beads. The non-imprinted polymer was synthesized by using the same procedure without the template molecule. The template was removed from the polymer matrix by washing *via* methanol and acetic acid (7:3, v/v). The washing procedure was repeated until the template was completely removed from the polymer.

Effect of contact time: In this study, a series of conical flasks containing 0.1 g of MIP and NIP were added with 10 mL of 10 ppm *p*-HBA solution. The conical flasks were agitated on a shaker at 250 rpm and the samples were collected at different time intervals of 30, 60, 90, 120, 150, 180, 210, 240, 270, 300, 330 and 360 min. The absorbance of the supernatant solution of *p*-HBA was recorded using UV spectrophotometry. The rebinding efficiency of polymers was calculated by:

$$\text{Extraction efficiency } (\%) = \frac{C_o - C_f}{C_o} \times 100 \quad (1)$$

where C_o is the initial absorbance and C_f is the final absorbance of *p*-HBA.

Effect of initial concentration: In this study, different initial concentrations (5, 10, 15, 20, 25 and 30 ppm) were tested. The amount of adsorbent and contact was 0.1 g and 210 min, respectively. The rebinding efficiency was calculated by eqn. 1 in all cases.

Effect of polymer dosage: The different masses of 0.1, 0.2, 0.3, 0.4 and 0.5 g of the MIP were placed in the different conical flasks and were added with 10 mL of 10 ppm *p*-HBA. The conical flasks were shaken at 250 rpm for 210 min. The rebinding efficiency was calculated by eqn. 1 in all cases.

Kinetic study: The rate and kinetic mechanism of *p*-HBA were examined in this work using the pseudo-first-order and pseudo-second-order kinetic models. The pseudo-first-order and pseudo-second-order linear equations are represented by eqns. 2 and 3, respectively. The best-fitting kinetic model that explains the adsorption of *p*-HBA was determined to be the one with a greater correlation coefficient (R^2).

Pseudo-first-order:

$$\log(q_e - q_t) = \log(q_e) - K_1\left(\frac{t}{2.303}\right) \quad (2)$$

In this context, q_e represents the quantity of *p*-HBA that has been adsorbed at equilibrium, while q_t indicates the amount of *p*-HBA adsorbed at a specific time. K_1 denotes the pseudo-first-order equilibrium rate constant and t refers to the time interval associated with the adsorption of *p*-HBA.

Pseudo-second-order:

$$\frac{t}{q_t} = \frac{1}{K_2(q_e)^2} + \frac{t}{q_e} \quad (3)$$

In this context, q_e represents the quantity of *p*-HBA adsorbed at equilibrium, while q_t denotes the quantity of *p*-HBA adsorbed at any specified time. K_2 is identified as the pseudo-second-order equilibrium rate constant and t refers to the time interval associated with the adsorption of *p*-HBA.

Adsorption isotherm study: The adsorption capacity and surface of the MIP were described in this study using Langmuir and Freundlich isotherm models. The linear equations for the Freundlich and Langmuir isotherm models are represented by eqns. 4 and 6, respectively. As the best-fitted isotherm model, only one model with a better correlation coefficient (R^2) was chosen.

Langmuir isotherm:

$$\frac{C_e}{q_e} = \frac{1}{q_{max}K_L} + \frac{C_e}{q_{max}} \quad (4)$$

where q_{max} is the maximum adsorption capacity of *p*-HBA; q_e is the quantity of *p*-HBA adsorbed at equilibrium time; C_e is the *p*-HBA concentration at equilibrium and K_L is the Langmuir constant. The R_L (parameter of equilibrium) was calculated by using eqn. 5:

$$R_L = \frac{1}{1+K_L C_e} \quad (5)$$

where K_L is the Langmuir constant and C_e is the *p*-HBA concentration at equilibrium.

Freundlich isotherm:

$$\ln(q_e) = \ln K_F + \frac{1}{n}(\ln C_e) \quad (6)$$

where n is the constant related to adsorption intensity, K_F is the maximum adsorption capacity of *p*-HBA, C_e is the *p*-HBA concentration at equilibrium and q_e is the amount of *p*-HBA adsorbed at equilibrium time.

Competitive binding assay: A selectivity test was conducted to evaluate the MIP of *p*-HBA as a sensing material. Benzoic acid was used as a competitive template with *p*-HBA. In this study, 5 mL *p*-HBA (10 ppm) and 5 mL of benzoic acid (10 ppm) were mixed in a conical flask containing 0.1 g of MIP. The NIP was treated in the same manner. The conical flask was shaken on the shaker at 250 rpm and the sample was collected at 210 min. The distribution ratios (mL g^{-1}) of *p*-HBA between the MIP and NIP were determined using eqn. 7:

Distribution ratio:

$$K_D = \frac{(C_i - C_f)V}{C_M} \quad (7)$$

where C_i is the initial *p*-HBA/benzoic acid in solution; C_f is the final concentration of *p*-HBA/benzoic acid; V is the volume of solvent and M is the mass of MIP/NIP used.

Selectivity coefficient for *p*-HBA relative to a binding competitor; benzoic acid for MIP and NIP was calculated by using eqn. 8:

Selectivity coefficient:

$$K_{sel}\left(\frac{MIP}{NIP}\right) = \frac{K_D\ p\text{-HBA}}{K_D\ \text{Benzoic acid}} \quad (8)$$

where K_D (*p*-HBA) is the distribution ratio of MIP/NIP for *p*-HBA and K_D (benzoic acid) is the distribution ratio of MIP/NIP for benzoic acid.

The relative selectivity coefficient (K°) was determined by the following equation:

$$K^o = \frac{K_{sel}\ MIP}{K_{sel}\ NIP} \quad (9)$$

where K_{sel} MIP and K_{sel} NIP are the selective coefficients.

Extraction of *p*-HBA from blood serum: Fresh human blood (10 mL), devoid of drugs, were obtained. Following whole blood collection, the blood was left undisturbed at room temperature to coagulate. After centrifuging the clot for 10 min at 7000 rpm, the serum-containing supernatant was obtained and kept in a refrigerator until the next experiment. Following that, distilled water was used to dilute the blood serum in 1:10 ratio. Then, 5 mL of 10 ppm *p*-HBA was added to 5 mL of diluted blood serum. A conical flask containing 10 mL of spiked blood serum was filled with approximately 0.4 g of chosen MIP. Following that, the identical process as described in the batch binding analysis was used.

RESULTS AND DISCUSSION

Synthesis of MIP and NIP: The synthesis was carried out by using the non-covalent precipitation polymerization method. Non-covalent approaches involve self-assembly through weak intermolecular interactions between the template and functional monomers [39]. The ratio between template/monomer/crosslinker is a very crucial part for producing better extraction performance and can also determine the stability of the formed complex [40]. In this study, the molar ratio of the template/monomer/crosslinker was 1:3:12, respectively. The functional monomer used in the synthesis was acrylic acid in which the carboxyl group of acid could create a hydrogen bond with the *p*-HBA. EDGMA was chosen as a crosslinker because it is widely used for controlling the morphology and stabilizing the molecular reaction site. Solvent also played an important role in the synthesis of MIPs for the accurate assembly of a template and the monomer. Acetonitrile, a polar aprotic solvent, can allow the template and monomer to develop polar contacts because to its physical and chemical properties [40]. In this way, a non-covalent interaction was established between the template and monomer.

Characterizations of MIP

SEM analysis: Scanning electron microscopy (SEM) (JEOL JSM-6390LA) was used to analyze the morphology. The shape and size were observed at a magnification of 10000x as shown in Fig. 1, which depicts the uniform spherical shape and size of the polymer particles. All the polymeric particles are micro range in size, which may be due to the use of precipitation polymerization technique by using a non-covalent imprinting approach [41]. The other reason could be the type and volume of solvent used, which are also important factors that could affect the surface morphology and the pore diameter [42]. This research confirmed that using acetonitrile as a solvent medium results in microporous and well-defined spherical polymer microparticles.

FTIR analysis: The FTIR (IRAffinity-1 SHIMADZU) was used to analyze the chemical structure of MIP particles. A broad peak at 3550-3200 cm^{-1} attributed to the stretching of O-H was observed in MIPs (Fig. 2). A strong and broad peak at 2979.18-2975.33 cm^{-1} are due to the vibration of C-H stretching from carboxylic acid functional group. A strong peak was observed at 1728.29-1727.33 cm^{-1}, which represents the vibration mode of C=O from the carboxylic acid. This peak indicates the presence of acrylic acid as monomer is important for the binding interaction in molecular imprinting technique. The vibration of C=C stretching was detected at 1641.49-1639.56 cm^{-1} and this confirms

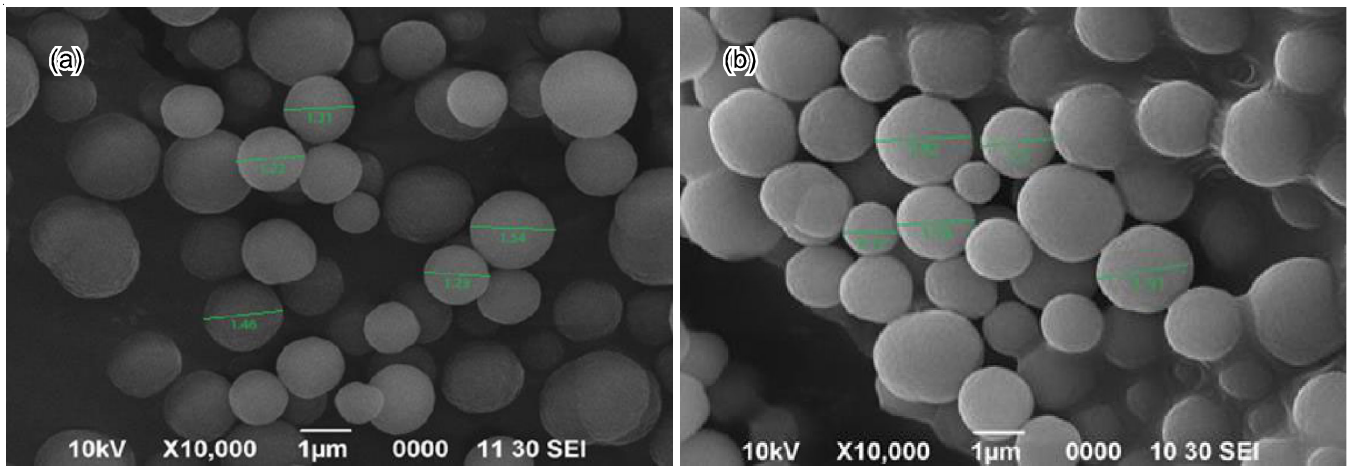

Fig. 1. SEM images of (a) MIP and (b) NIP

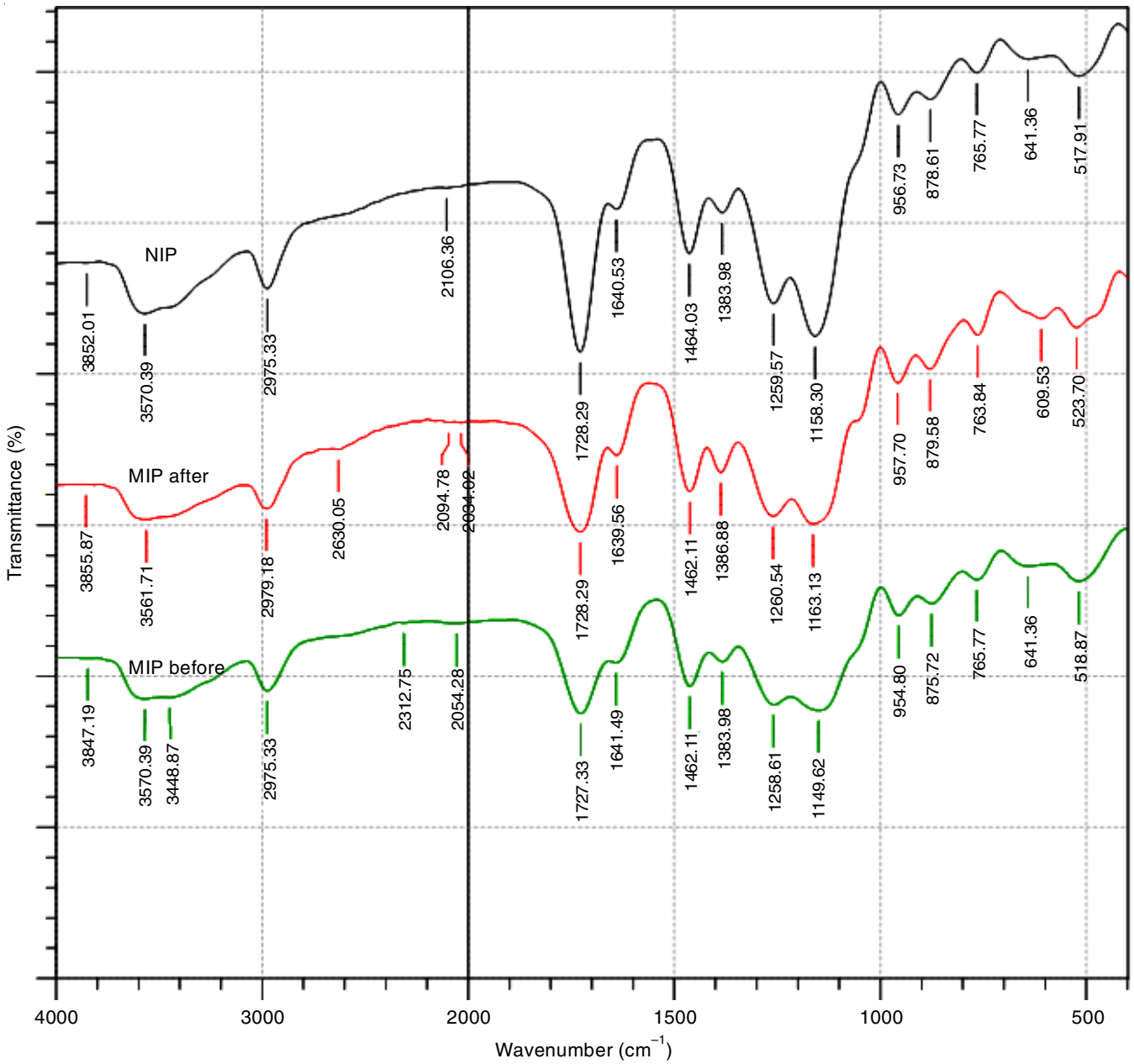

Fig. 2. FTIR spectra of MIP before wash, MIP after wash and NIP

the polymerization of monomers. The C-H bending at 1464.03-1462.11 and 879.58-875.72 cm^{-1} represent the presence of alkane. The strong peaks between 1000 cm^{-1} to 850 cm^{-1} are due to the bending of =C-H.

Batch binding assay: This assay was carried out to evaluate the best suitable contact time between template and polymer to have a higher rebinding efficiency. The higher affinity and rebinding efficiency towards the target analyte and greater number of recognition sites are crucial for MIP. From Fig. 3, it is clear that MIP has highest rebinding efficiency compared to the NIP. As for the NIP, the binding affinity is less as compared to the MIP. This is due to the presence of recognition sites in the MIP, which lacked in NIP [43-45]. Moreover, it is also observed that with the increase in the contact time during the binding process, there is an increase in the adsorption of the target analyte onto the synthesized polymeric surface until the equilibrium is attained at 210 min after that a decrease in adsorption was observed. The highest rebinding efficiency of 76.01% was achieved at 210 min. The optimum and efficient time for the MIP to rebind the *p*-HBA was at 210 min.

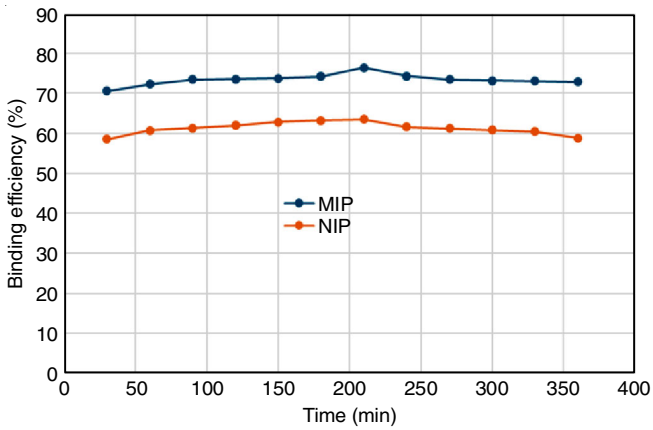

Fig. 3. Binding efficiency (%) at different time interval

Effect of different template concentration: The rebinding affinity of the template depends on the available recognition sites. Initially the rebinding of template increases with the increase in concentration until it reaches a certain point to have higher rebinding efficiency (Fig. 4). After this optimum point it started decreasing and this may be due to the saturation of template molecules around the binding sites of MIP [43-45]. A 10 ppm was considered as the optimum concentration for the highest rebinding efficiency of MIP.

Effect of MIP dosage: The effect of MIP dosage on the rebinding efficiency is shown in Fig. 5. With the increase in the amount of MIP the number of recognition sites will also increase. The results of this study showed that with the increase in the dosage of polymer the rebinding efficiency also increased until it reached an optimum amount of 0.4 g. The further increase in the amount of MIP has shown a decreasing trend this may be due to the aggregation of MIP particles resulting in the hindrance towards the binding sites [43-45].

Kinetic studies: Fig. 6 displayed the pseudo-first-order kinetic model and the pseudo-second-order kinetic model of *p*-HBA with R^2 value of 0.5311 and 0.9457, respectively. The

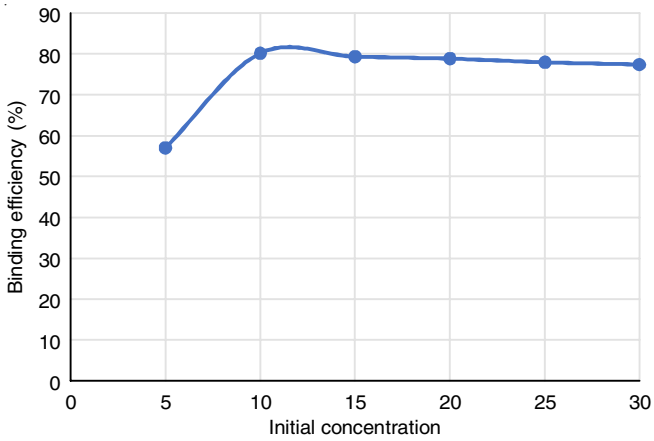

Fig. 4. Rebinding efficiency (%) of MIP at different template concentrations

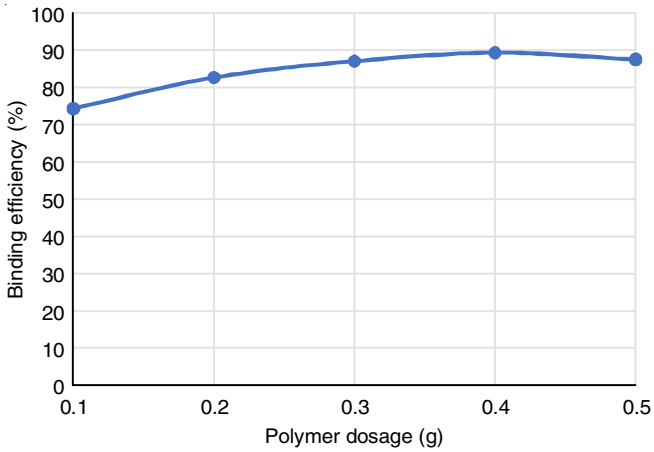

Fig. 5. Binding efficiency (%) of MIP of different amount of MIP

pseudo-second-order kinetic model is the best kinetic model for the adsorption process due to the higher R^2 value, which indicated that the adsorption process is the chemisorption. This suggests that chemisorption dominates the adsorption process, involving the valence forces or electron sharing.

Adsorption isotherms: In this study, both Langmuir and Freundlich isotherm models were applied on *p*-HBA to determine the adsorption mechanism and extent of *p*-HBA adsorbed on the MIP surface. The results depicted in Fig. 7 showed the relationship between *p*-HBA and MIP in the form of Langmuir and Freundlich isotherm models, respectively. Moreover, the values of Langmuir constants (q_{max}, K_L and R_L) and their correlation coefficient (R^2), as well as the Freundlich constants (K_F, n and 1/n) and their correlation coefficient (R^2) are displayed in Table-1. The adsorption process was concluded on the basis of R^2 value. The Freundlich isotherm model showed the highest R^2 value. This indicated the multi-layer mechanism of adsorption occurs in MIP with heterogeneous binding sites.

Competitive batch binding assay: This assay was tested to evaluate the properties of MIP recognition site of *p*-HBA as sensing material [30]. The selected competitor was benzoic acid, which is the structural analogue of *p*-HBA. Based on Table-2, the distribution ratio of K_D MIP of *p*-HBA is higher than K_D MIP of benzoic acid. It showed that the sensing properties of MIP towards the *p*-HBA, which means that the recognition sites in MIP are more complementary with *p*-HBA as compared

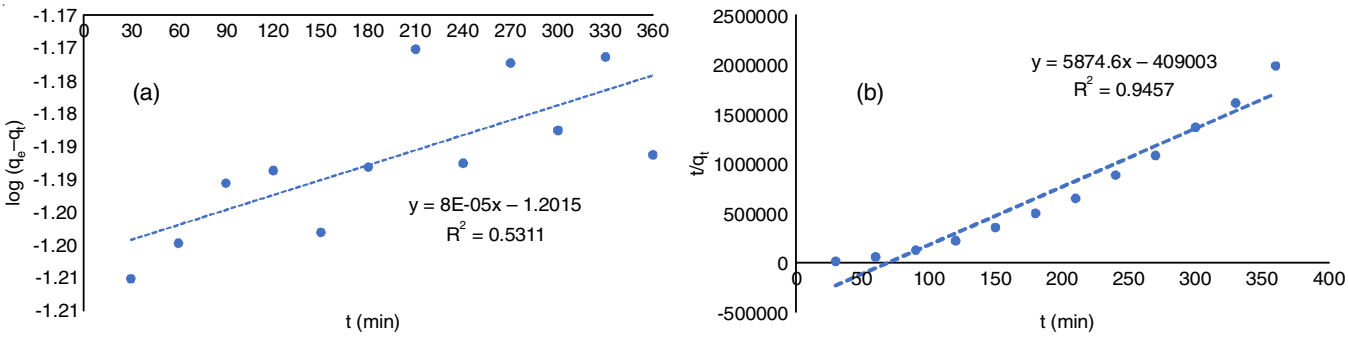

Fig. 6. (a) Pseudo-first-order and (b) pseudo-second-order kinetic model of MIP

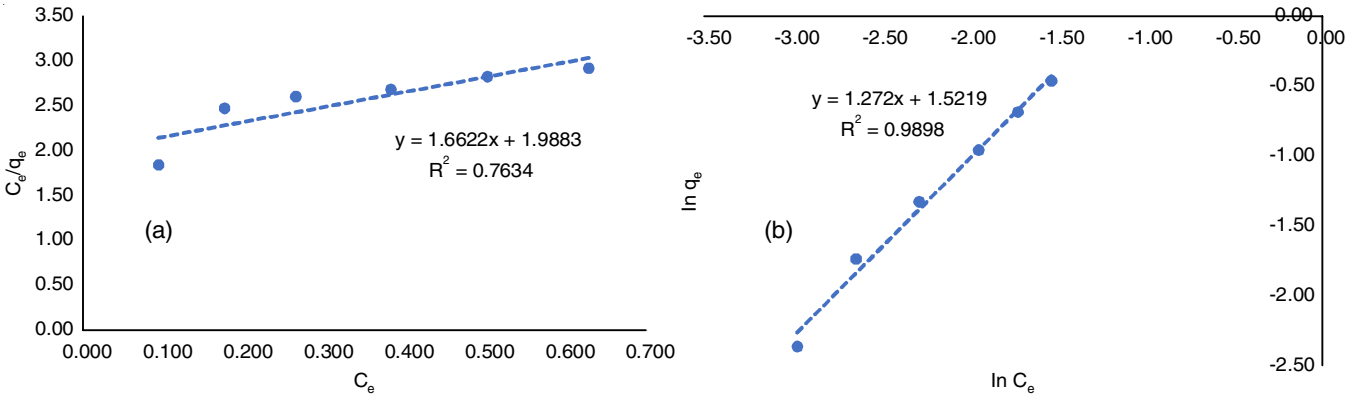

Fig. 7. (a) Langmuir isotherm model and (b) Freundlich isotherm model of MIP

TABLE-1
VALUES OF ADSORPTION ISOTHERM MODELS

Langmuir constants				Freundlich constants			
q_{max}	K_L	R_L	R^2	K_F	n	1/n	R^2
0.6016	0.8360	0.3671	0.7634	4.5809	0.7862	1.272	0.9898

TABLE-2
THE DISTRIBUTION RATIO, SELECTIVITY COEFFICIENTS AND RELATIVE SELECTIVITY COEFFICIENT OF MIP AND NIP

	K_D MIP (MAA)	K_D NIP (MAA)	K_{sel}	k′
p-HBA (template molecule)	80.57	70.62	1.70	–
Benzoic acid (competitive compound)	47.48	46.68	1.51	1.13

to benzoic acid. The higher selectivity coefficient of *p*-HBA also indicated the complimentary binding in MIP as compared to the NIP.

Extraction of *p*-HBA from spiked blood serum: The extraction of *p*-HBA was tested in spiked blood serum sample. A good amount of *p*-HBA was extracted from the blood sample. The extraction efficiency of MIP was about 80.56% and at the same time was tested using NIP which was about 56.58%. This proved that the synthesized MIP has specific binding sites for the template molecule.

Conclusion

The molecular imprinted polymer of *p*-hydroxybenzoic acid (*p*-HBA) was synthesized by using precipitation polymerization with suitable recognition sites. This was obvious from the competitive binding that the molecularly imprinted polymer (MIP) showed higher affinity towards *p*-HBA as compared to benzoic acid. An appreciable amount of 80% *p*-HBA was extracted from the blood serum sample. The relative selectivity coefficient (1.13) indicated the potential application of synthesized MIP for selective extraction of *p*-HBA from mixture of compounds. This will provide an opportunity for the use of this kind of material in the solid phase extraction in the complex matrix samples.

ACKNOWLEDGEMENTS

The authors acknowledged the financial support from the IMPACT Research Grant Scheme through the Research Grant F07/PARTNERS/2115/202.

CONFLICT OF INTEREST

The authors declare that there is no conflict of interests regarding the publication of this article.

REFERENCES

1. C. Li, Y. Deng, J. Wang, W. Ruan, S. Wang and W. Kong, *Sustainability*, **15**, 9285 (2023); https://doi.org/10.3390/su15129285s
2. C.J. Gao and K. Kannan, *Environ. Int.*, **136**, 105465 (2020); https://doi.org/10.1016/j.envint.2020.105465
3. H.Z. Castada, Z. Sun, S.A. Barringer and X. Huang, *J. Am. Oil Chem. Soc.*, **97**, 289 (2020); https://doi.org/10.1002/aocs.12331
4. J.L. Wang and Z.G. Jiang, *Int. J. Food Sci. Technol.*, **57**, 1283 (2022); https://doi.org/10.1111/ijfs.15518
5. Y. Wang, C. Li, Q. Wang, H. Wang, B. Duan and G. Zhang, *J. Soils Sediments*, **16**, 1858 (2016); https://doi.org/10.1007/s11368-016-1375-8
6. C.Y. Liao, J.B. Shi, X.Y. Wang, Q.Q. Zhu and K. Kannan, *Environ. Pollut.*, **253**, 759 (2019); https://doi.org/10.1016/j.envpol.2019.07.076
7. A.L. Ball, M.E. Solan, M.E. Franco and R. Lavado, *Drug Chem. Toxicol.*, **46**, 786 (2022); https://doi.org/10.1080/01480545.2022.2100900
8. M.I. Hussain and M.J. Reigosa, *Biomolecules*, **11**, 233 (2021); https://doi.org/10.3390/biom11020233
9. M. Nobile, F. Arioli, R. Pavlovic, F. Ceriani, S.K. Lin, S. Panseri, R. Villa and L.M. Chiesa, *Food Addit. Contam. Part A Chem. Anal. Control Expo. Risk Assess.*, **37**, 131 (2020); https://doi.org/10.1080/19440049.2019.1682686
10. L. Wang, Y.H. Wu, W. Zhang and K. Kannan, *Environ. Sci. Technol.*, **47**, 2069 (2013); https://doi.org/10.1021/es304659r
11. L.H. Chen, X.M. Yang, W. Raza, J.H. Li, Y.X. Liu, M.H. Qiu, F.G. Zhang and Q.R. Shen, *Appl. Microbiol. Biotechnol.*, **89**, 1653 (2011); https://doi.org/10.1007/s00253-010-2948-x
12. A. Scavo, C. Abbate and G. Mauromicale, *Plant Soil*, **442**, 23 (2019); https://doi.org/10.1007/s11104-019-04190-y
13. W.Y. Hao, L.X. Ren, W. Ran and Q.R. Shen, *Plant Soil*, **336**, 485 (2010); https://doi.org/10.1007/s11104-010-0505-0
14. Q. Liu, X. Sun, L. Zhang, K. Li, X. Guo, Y. Guo and Z. Liu, *Sci. Hortic.*, **256**, 108541 (2019); https://doi.org/10.1016/j.scienta.2019.05.068
15. Z.Z. Zhang, Z.D. Zhang, X.Y. Han, J.H. Wu, L.Z. Zhang, J.R. Wang and G. Wang-Pruski, *Ecotoxicol. Environ. Saf.*, **200**, 110779 (2020); https://doi.org/10.1016/j.ecoenv.2020.110779
16. A. Muscolo, M.R. Panuccio and M. Sidari, *Plant Growth Regul.*, **35**, 31 (2001); https://doi.org/10.1023/A:1013897321852
17. E.K. Lim, C.J. Doucet, Y. Li, L. Elias, D. Worrall, S.P. Spencer, J. Ross and D.J. Bowles, *J. Biol. Chem.*, **277**, 586 (2002); https://doi.org/10.1074/jbc.M109287200
18. T.L. Weir, S.W. Park and J.M. Vivanco, *Curr. Opin. Plant Biol.*, **7**, 472 (2004); https://doi.org/10.1016/j.pbi.2004.05.007
19. Y. Zhang, M. Gu, K. Shi, Y.H. Zhou and J.Q. Yu, *Plant Soil*, **327**, 455 (2010); https://doi.org/10.1007/s11104-009-0075-1
20. C. Huang, L. Xu, S. Jin-jing, Z. Zhang, M. Fu, H. Teng and K. Yi, *J. Integr. Agric.*, **19**, 518 (2020); https://doi.org/10.1016/S2095-3119(19)62781-4
21. G.T. Liang, J. Guo, S.Y. Zhang and G.C. Zhang, *J. For. Res.*, **32**, 2155 (2021); https://doi.org/10.1007/s11676-020-01107-9
22. E. Blanco, M.D. Casais, M.D. Mejuto and R. Cela, *Anal. Chim. Acta*, **647**, 104 (2009); https://doi.org/10.1016/j.aca.2009.05.024
23. F.Z. Kashani, S.M. Ghoreishi, A. Khoobi and M.A. Enhessari, *Mikrochim. Acta*, **186**, 12 (2019); https://doi.org/10.1007/s00604-018-3113-y
24. E. Hoberg, B. Meier and O. Sticher, *Phytochem. Anal.*, **11**, 327 (2000); https://doi.org/10.1002/1099-1565(200009/10)11:5<327::AID-PCA523>3.0.CO;2-0
25. Y. Shi, J. Zhang, J. He, D. Liu, X. Meng, T. Huang and H.A. He, *Talanta*, **191**, 133 (2019); https://doi.org/10.1016/j.talanta.2018.08.036
26. P. Cherian, J. Zhu, W.F. Bergfeld, D. Belsito, R.A. Hill, C.D. Klaassen, D.C. Liebler, J.G. Marks Jr., R.C. Shank, T.J. Slaga, P.W. Snyder and B. Heldreth, *Int. J. Toxicol.*, **39(S1)**, 5S (2020); https://doi.org/10.1177/1091581820925001
27. B.W. Sun, Y.Z. Li and W.B. Chang, *J. Mol. Recognit.*, **14**, 388 (2001); https://doi.org/10.1002/jmr.550
28. C. Michailof, P. Manesiotis and C. Panayiotou, *J. Chromatogr. A*, **1182**, 25 (2008); https://doi.org/10.1016/j.chroma.2008.01.001
29. H.-R. Park, S.-D. Yoon, J.-C. Lee and S.-H. Chough, *J. Appl. Polym. Sci.*, **105**, 2824 (2007); https://doi.org/10.1002/app.26265
30. A. Beltran, R.M. Marcé, P.A.G. Cormack and F. Borrull, *Anal. Chim. Acta*, **677**, 72 (2010); https://doi.org/10.1016/j.aca.2010.07.021
31. Y. Dong, P. Yu, Q. Sun, Y. Lu, Z. Tan and X. Yu, *Chem. Res. Chin. Univ.*, **34**, 1051 (2018); https://doi.org/10.1007/s40242-018-8146-6
32. G. Zhu, G. Cheng, P. Wang, W. Li, Y. Wang and J. Fan, *Talanta*, **200**, 307 (2019); https://doi.org/10.1016/j.talanta.2019.03.070
33. T. Sajini and B. Mathew, *Talanta Open*, **4**, 100072 (2021); https://doi.org/10.1016/j.talo.2021.100072
34. N.A. Yusof, A. Beyan and N.A. Ibrahim, *Sains Malays.*, **39**, 829 (2010).
35. R.M. Roland and S.A. Bhawani, *J. Anal. Methods Chem.*, **2016**, 1 (2016); https://doi.org/10.1155/2016/5671507
36. R.M. Roland and S.A. Bhawani, *Asian J. Chem.*, **31**, 2770 (2019); https://doi.org/10.14233/ajchem.2019.22243
37. R.M. Roland, S.A. Bhawani, R. Wahi and M.N.M. Ibrahim, *J. Liq. Chromatogr. Relat. Technol.*, **43**, 94 (2020); https://doi.org/10.1080/10826076.2019.1672077
38. E.N. Zare, Z. Fallah, V.T. Le, V. Doan, A. Mudhoo, S. Joo, Y. Vasseghian, M. Tajbakhsh, O. Moradi, M. Sillanpää and R.S. Varma, *Environ. Chem. Lett.*, **20**, 2629 (2022); https://doi.org/10.1007/s10311-022-01439-4
39. E. Caro, N. Masqué, R.M. Marce, F. Borrull, P.A.G. Cormack and D.C. Sherrington, *J. Chromatogr. A*, **963**, 169 (2002); https://doi.org/10.1016/S0021-9673(02)00360-6
40. M.A. García Mayor, G. Paniagua González, R.M. Garcinuño Martínez, P. Fernández Hernando and J.S. Durand Alegría, *Food Chem.*, **221**, 721 (2017); https://doi.org/10.1016/j.foodchem.2016.11.114
41. F.G. Tamayo, J.L. Casillas and A. Martin-esteban, *J. Chromatogr. A*, **1069**, 173 (2005); https://doi.org/10.1016/j.chroma.2005.02.029
42. G.P. González, P.F. Hernando and J.S.D. Alegría, *Anal. Chim. Acta*, **557**, 179 (2006); https://doi.org/10.1016/j.aca.2005.10.034
43. R.M. Roland, S.A. Bhawani, M.N.M. Ibrahim and R. Wahi, *ChemistrySelect*, **9**, e202303679 (2024); https://doi.org/10.1002/slct.202303679
44. R.M. Roland, S.A. Bhawani and M.N.M. Ibrahim, *BMC Chem.*, **17**, 165 (2023); https://doi.org/10.1186/s13065-023-01084-0
45. R.M. Roland, S.A. Bhawani and M.N.M. Ibrahim, *Chem. Biol. Technol. Agric.*, **10**, 92 (2023); https://doi.org/10.1186/s40538-023-00462-z